THE ASTRONOMICAL JOURNAL VOLUME 113, NUMBER 3 MARCH 1997

THE H I-RICH ELLIPTICAL GALAXY NGC 5266[1]

R. MORGANTI
CSIRO, Australia Telescope National Facility, PO Box 76, Epping, NSW 2121, Australia; and Istituto di Radioastronomia, CNR, via Gobetti 101, 40129 Bologna, Italy
Electronic mail: rmorgant@atnf.csiro.au

E. M. SADLER
School of Physics, University of Sydney, NSW 2006, Australia
Electronic mail: ems@physics.sa.oz.au

T. OOSTERLOO
CSIRO, Australia Telescope National Facility, PO Box 76, Epping, NSW 2121, Australia
Electronic mail: toosterl@atnf.csiro.au

A. PIZZELLA AND F. BERTOLA
Dipartimento di Astronomia, Vicolo dell'Osservatorio 5, 35122 Padova, Italy
Received 1996 July 8; revised 1995 November 26
Electronic mail: pizzella@astrpol.astro.it, bertola@astrpol.astro.it

ABSTRACT

We present new H I images of the dust-lane elliptical galaxy NGC 5266 already known from single-dish observations to contain a large amount of H I. Our new data confirm that NGC 5266 contains $\sim 2.4\times10^{10}$ $M_\odot$ (for $H_0=50$ km s^{-1} Mpc^{-1}) of neutral hydrogen, i.e., more than most spiral galaxies of similar luminosity. The gas extends to $\sim 8'$ each side of the nucleus, or 8 times the optical half-light radius R_e. Surprisingly, most of the H I extends almost orthogonal to the optical dust lane. A small fraction of the H I is associated with the dust lane and there are some hints of a faint warp connecting the two structures. The H I distribution is somewhat clumpy and asymmetric, but the overall velocity field in the inner $4'$ can be successfully modeled by assuming that the gas lies mainly in two perpendicular planes—in the plane of the dust lane in the central parts and orthogonal to this in the outer regions. Beyond the $4'$ radius, the gas has a different structure and may be in two tidal tails, or an edge-on ring. Measurement of the H I rotation curve is affected by asymmetries in the gas distribution, but the rotation velocity is at least 250 km s^{-1} at a radius of $4'$, and a flat rotation curve of ~ 270 km s^{-1} is consistent with the data. This would imply a value of $M/L_B\sim 8$ at ~ 4 R_e. If the outermost H I is in an edge-on ring, we estimate $M/L_B\sim 16$ at ~ 8 R_e. Comparing this with the value derived from optical observations for the inner region we find an increase of M/L_B by a factor ~ 2.7 at $r\sim 4$ R_e, and by 5.3 at $r\sim 8$ R_e. The large amount of neutral gas observed in NGC 5266 ($M_{HI}/L_B\sim 0.2$) and the H I morphology, suggest that this object may have formed from the merger of two spiral galaxies. If so, NGC 5266 probably represents a relatively old merger remnant since most of the H I gas appears settled. © *1997 American Astronomical Society.*
[S0004-6256(97)00803-0]

1. INTRODUCTION

The H I distribution and velocity field can, in principle, provide a powerful tool for studying the intrinsic shape and internal dynamics of a galaxy and measuring the radial variation of M/L. This is especially true when the H I gas extends well beyond the optical galaxy. Only a few elliptical galaxies are known to contain large amounts ($>5\times10^9$ $M_\odot$) of H I and since the number of such galaxies remains small despite of sensitive searches with radio telescopes, such objects must be rare. Very extended H I has been detected in only a handful of elliptical galaxies (see van Gorkom 1992 for references).

By comparing the central M/L values (from stellar velocity dispersions or the kinematics of ionized gas) to those at large radii from H I, Bertola *et al.* (1993) produced evidence for dark-matter halos around elliptical galaxies. These authors suggest that spiral and elliptical galaxies could have similar radial M/L profiles if distances from the center are expressed in terms of optical half-light radius R_e: for both types M/L is approximately constant out to 1–2 R_e, then starts to increase further out. However, the systematics of dark-matter content in early-type galaxies with other parameters like luminosity is still unclear and more data are needed

[1]Based on observations with the Australia Telescope Compact Array (ATCA), which is operated by the CSIRO Australia Telescope National Facility.

 0004-6256/97/113(3)/937/13/$10.00

to address this question (see de Zeeuw & Franx 1991 and de Zeeuw 1992 for a review).

Another open question is the extent to which infall of neutral gas might fuel nuclear activity. Knapp (1986) found for high luminosity ellipticals that the observed presence of H I significantly enhances the likelihood that the galaxy is a radio source (see also van Gorkom 1992), and infalling cold gas has been observed in a number of radio ellipticals (van Gorkom *et al.* 1989). Dust lanes also hint at a relationship between cold gas and radio activity. It has been suggested that galaxies with dust lanes more often have a radio detection than dustless galaxies (Sadler & Gerhard 1985) and dust lanes tend to lie perpendicular to radio jets (Kotanyi & Ekers 1979; Möllenhoff *et al.* 1992; van Dokkum & Franx 1995) indicating that the rotation axis of the gas and the radio jets are aligned. However, Möllenhof *et al.* 1992 found several exceptions to this rule, and there are also ellipticals with H I which do not appear to have an active nucleus.

Here, we present new H I observations of the dust-lane elliptical galaxy NGC 5266. This galaxy was known from single-dish observations to contain a large amount of neutral hydrogen (Varnas *et al.* 1987), and it has also been studied in detail optically (Caldwell 1984; Varnas *et al.* 1987), making it an ideal candidate with which to investigate the questions discussed above.

The paper is organized as follows: Section 2 summarizes previous work on NGC 5266; Sec. 3 describes our Australia Telescope Compact Array (ATCA) observations and presents new H I and radio continuum data for NGC 5266 and several neighboring galaxies. In Sec. 4 we discuss the results of the H I observations and present a simple model for the gas distribution in NGC 5266. The implications for M/L and the presence of dark matter are also discussed. Finally, in Sec. 5, we discuss the possible origin of the neutral gas.

2. BASIC PROPERTIES OF NGC 5266

NGC 5266 is a bright E4 elliptical galaxy with a prominent dust lane along its projected minor axis. Except for the presence of the dust lane, the surface brightness distribution follows a de Vaucouleur law essentially perfectly (Varnas *et al.* 1987). Its systemic velocity is $V_{\rm hel}$=3044 km s^{-1} for the stellar component and 2994 km s^{-1} for the ionized gas (Varnas *et al.* 1987), and we adopt [2] a distance of 60 Mpc. Optical images of the galaxy and its dust lane can be found in Varnas *et al.* and Caldwell (1984).

Optically, the galaxy has been studied in detail by several authors. Caldwell (1984) measured the velocity field of both the dust lane (seen almost edge-on) and the stellar galaxy, and found that the stars rotate about the optical minor axis while the gas in the dust lane rotates about the optical major axis (with a maximum rotation velocity of $\sim$260 km s^{-1}), i.e., the kinematic axes of the stars and gas appear orthogonal. The stellar rotation is more rapid than in most bright ellipticals (maximum rotation velocity $\sim$ 210 km s^{-1}). The dust lane has a 25° warp which is rotating in a prograde sense to the stellar rotation and is therefore not in a plane stable against precession. As a result, Caldwell (1984) suggested that the underlying galaxy is triaxial and the warp is the result of to incomplete settling of the gas in a stationary potential.

[2]We use H_0=50 km s^{-1} Mpc^{-1} throughout this paper.

TABLE 1. Properties of NGC 5266.

			Ref.
Position (J2000.0)	$13^h43^m01^s.7$	$-48°10'12''$	a
Distance	60	Mpc	
Angular scale	17.4	kpc/arcmin	
M_B	−22.40	mag	a
L_B	1.4×10^{11}	$L_\odot$	a
$M_{\rm HI}$	1.8×10^{10}	$M_\odot$	b
$M_{\rm HI}$	2.4×10^{10}	$M_\odot$	c
$M_{\rm H_2}$	2.7×10^{9}	$M_\odot$	d

References: (a) de Vaucouleurs *et al.* 1991, (b) Varnas *et al.* 1987, (c) this paper, (d) Sage & Galletta 1993.

Varnas *et al.* (1987) made further velocity measurements of NGC 5266 and found some stellar rotation about the galaxy's major axis, so that the kinematic and photometric axes are misaligned—again implying that the underlying galaxy is triaxial. Using these data they showed that a triaxial model slowly tumbling in a retrograde direction with respect to the observed stellar stream can reproduce a warped disk, which cannot be achieved (according to their model) with the model proposed by Caldwell (1984). From dynamical modeling, they deduced that the ionized gas has settled onto stable orbits and is not a recent acquisition. They also detected H I in NGC 5266 using the Parkes 64 m radio telescope and found that the galaxy contains around $1.8\times10^{10}M_\odot$ of neutral hydrogen, one of the largest amounts observed in any elliptical galaxy.

Goudfrooij *et al.* (1994) used photometry of NGC 5266 to study the dust content and extinction and estimated a total dust mass of $2\times10^6M_\odot$, slightly lower than the 5–6 $\times10^6M_\odot$ implied by *IRAS* measurements (Roberts *et al.* 1991). From narrow-band imaging in the Hα and [N II] lines, they showed that the ionized gas in NGC 5266 lies in a ring, rather than in a disk as assumed by Caldwell (1984) and Varnas *et al.* (1987). The ring of ionized gas is clearly associated with the dust ring.

Sage & Galletta (1993) made CO observations of NGC 5266 and found that the molecular gas also has a ring-like distribution and is co-rotating with the ionized gas. The width of the CO profile suggests rotation speeds of about 270–300 km s^{-1} within the central arcminute, and the H_2 mass estimated from the CO observations is $2.7\times10^9M_\odot$ (using the standard conversion from CO flux to H_2 mass, Solomon *et al.* 1987). Table 1 summarizes some observed properties of NGC 5266.

3. THE RADIO OBSERVATIONS

The high H I content and regular global H I profile of NGC 5266 make it a good candidate for H I mapping. Since it is necessary to make observations which are sensitive to extended emission, but also have high enough resolution to allow some modeling of the velocity field, we combined observations with four different configurations of the ATCA.

TABLE 2. ATCA observations.

Date	Configuration	Baseline range (m)	Frequency (MHz)	Time
Apr 94	375	31–337	1406	2×12 h
May 94	1.5D	107–1439	1406	12 h
Apr 95	1.5A	152–1316	1406	2×12 h
			1344	
May 95	1.5B	31–1286	1406	12 h
			2378	

The 375 m configuration (one of the most compact ATCA configurations) gives maximum sensitivity to extended, low surface-brightness emission with a resolution of about 2′. The higher spatial resolution needed for a detailed kinematical study, especially in the region coincident with the dust lane, was achieved by combining three 1.5 km configurations (resolution ~30″) to give a uniform *uv* coverage. Table 2 summarizes our observations.

In the first two observing runs, we used a 16 MHz bandwidth with 512 channels. Hanning smoothing in frequency was applied to the *uv* data giving a final velocity resolution of 12.4 km s^{-1}. In the last two runs we used 256 channels (again with 16 MHz bandwidth) and we did not apply any smoothing. In both cases the band was centered at the optical velocity of 3044 km s^{-1}.

The correlator configuration used in the second set of observations allowed us to use a second IF for simultaneous continuum observations with a bandwidth of 128 MHz and 33 channels. We used a central continuum wavelength of 1344 MHz (20 cm) in the 1995 April run and 2378 MHz (13 cm) in 1995 May.

In each run we observed NGC 5266 for ~12 h, with calibrators (1329–665 and 1313–333) observed every hour to monitor gain changes. The flux-density scale was set by observations of 1934–638, for which we adopted a flux density of 14.9 Jy at 1400 MHz and 12.2 Jy at 2378 MHz. This source was also used as a bandpass calibrator.

Table 3 summarizes the instrumental parameters of the line and continuum observations.

3.1 Neutral Hydrogen Data

The spectral data were calibrated with the MIRIAD package (Sault *et al.* 1995), which has a number of features particularly suited for ATCA data. The continuum subtraction was also done in MIRIAD by using a linear fit through the line-free channels of each visibility record and subtracting this fit from all the frequency channels. The continuum emission of NGC 5266 was already known to be weak (<30 mJy at 2.7 GHz; Sadler 1984a), and caused no problems for the line data. After calibration and continuum subtraction, the data from the different runs were combined and the final reduction (i.e., CLEAN and moment analysis of the data cube) was done with GIPSY (Allen *et al.* 1985). The combined data cube made with natural weighting has an rms noise of 0.81 mJy beam^{-1} and a resolution of 60×30″ (P.A. 19).

As expected from the width of the single-dish profile (Varnas *et al.* 1987), we detect H I emission over a wide velocity range from ~2750 to ~3350 km s^{-1}. Figure 1 shows the total H I profile measured with the ATCA. An interference spike generated by the data acquisition system is present at 1408 MHz, corresponding to a velocity of ~2644 km, but this did not affect the detection of low-velocity gas in NGC 5266. Figure 2 shows maps of the individual velocity channels (plotted every second channel).

TABLE 3. Instrumental parameters of the ATCA observations.

H I observations	
Field Center (J2000.0)	$13^h43^m01^s.6$ −48°10′12″
Synthesized beam (nat. weight)	60″×30″, P.A.=19°
Number of channels	256
Velocity of the band center (km s^{-1})	3044
Velocity resolution (km s^{-1})	12.4
rms noise in channel maps (mJy beam^{-1})	0.81
Peak of the emission (mJy)	120.3
Continuum 1344 MHz	
Synthesized beam (unif. weight)	29.8″×14.6″, P.A.=15.8°
rms noise (mJy beam^{-1})	0.16
Peak of the emission (mJy)	12.3
Continuum 2378 MHz	
Synthesized beam (unif. weight)	13.5″×13.5″, P.A.=10.5°
rms noise (mJy beam^{-1})	0.08
Peak of the emission (mJy)	6.4

We estimate a total H I mass of $2.4\times10^{10}M_\odot$ for NGC 5266. This is consistent with the Parkes single-dish measurements made by Varnas *et al.* (1987) considering that the extent of the H I in NGC 5266 is larger than the 15′ diameter of the Parkes beam at 21 cm, (see below) which could explain why the H I mass derived from the ATCA data is slightly higher than that from the single-dish data. The velocity centroid of the H I is at ~2990 km s^{-1}, with a width (at 20%-level) of ~650 km s^{-1}.

The total intensity and the intensity-weighted mean velocity of the H I emission were derived from a data cube produced in the following way (van Gorkom & Ekers 1989). The original data cube was smoothed spatially to a resolution of 90″×60″. The smoothed cube was used to mask the original cube: pixels with signal below 2σ in the smoothed cube

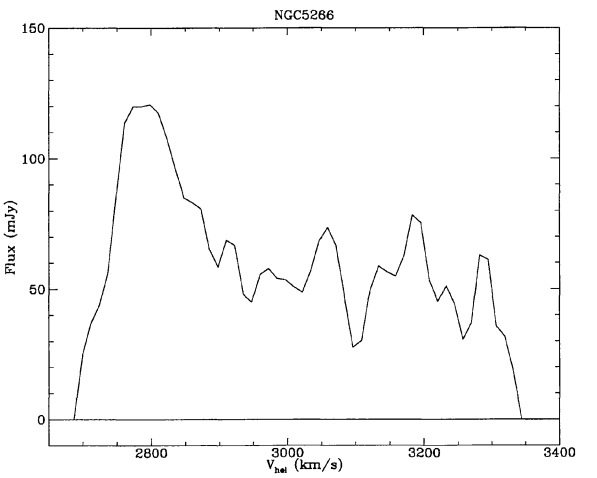

FIG. 1. The total H I profile of NGC 5266 from the ATCA data.

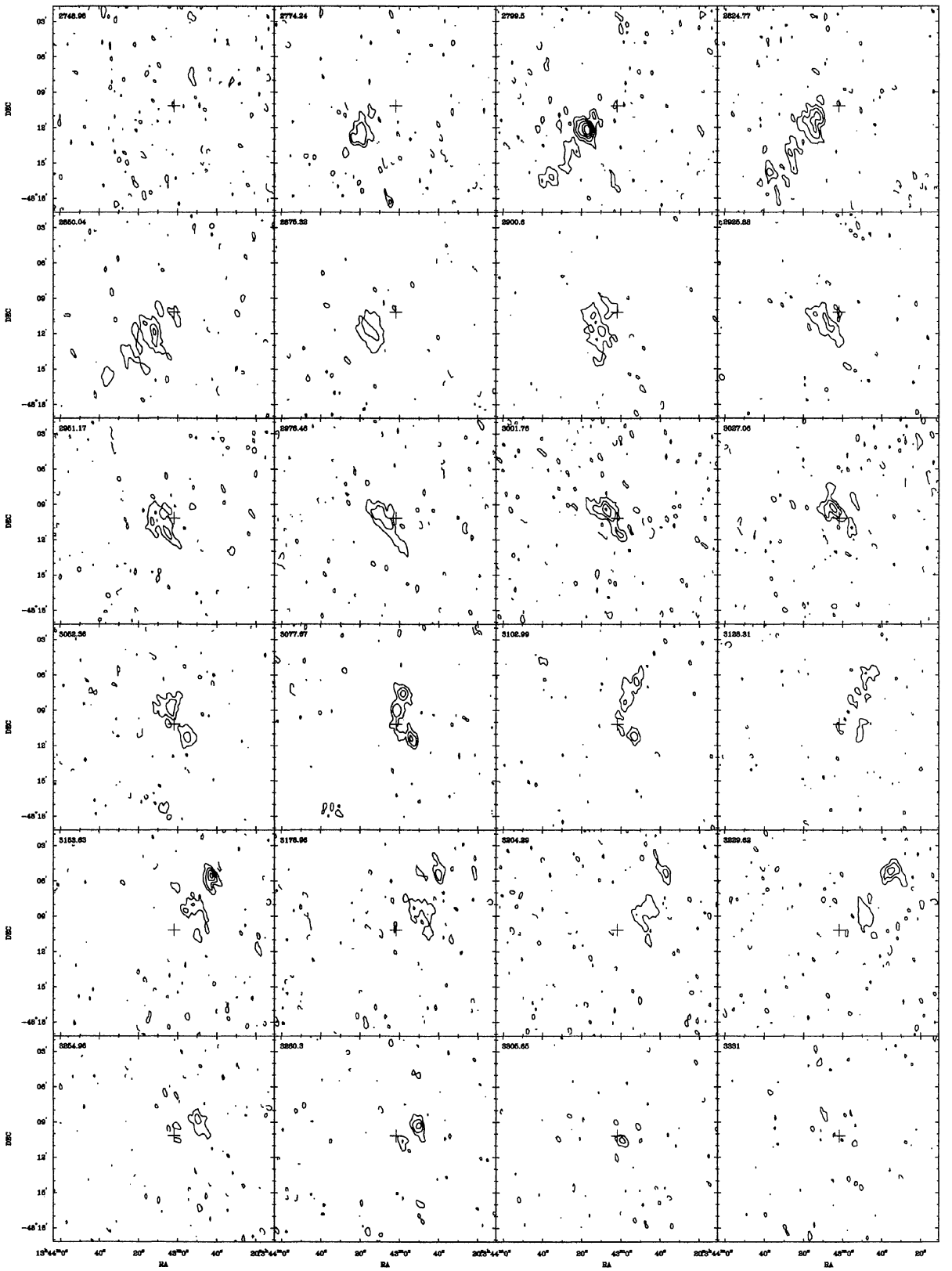

FIG. 2. Individual channel maps (plotted every second channel) of the H I distribution in NGC 5266. Contour level are $2\times$ −1,1,2,3,4,5,6,7,8,9 mJy beam^{-1}. The cross indicates the optical position and the velocity value of each channel is also given.

TABLE 4. Continuum emission from NGC 5266.

Freq. (Ghz)	Flux density (mJy)	rms noise (mJy/beam)	Resolution (arcsec)
1.3	12.3±0.9	0.16	29.8×14.6
2.4	6.4±0.6	0.08	13.5×10.5
2.4*	6.9±0.6	0.10	29.8×14.6

*Spatial resolution degraded to match 1.3 GHz observation.

were set to zero in the original cube. Moreover, only points with unmasked signal in at least two consecutive channels were used in the moment analysis.

3.2 Continuum Data

The continuum data were also reduced in MIRIAD, and Table 4 summarizes the results.

At both 1.3 and 2.4 GHz, there is a single point source coincident with the optical nucleus. This continuum source was also detected by Harnett (1987), who measured a flux density of 20 mJy at 843 MHz. The source has a rather steep spectral index ($\alpha \sim -1.1$ for $S \sim \nu^{\alpha}$), and the flux density, measured on a 2.4 GHz map made with the same beam as the 1.3 GHz observations (see Table 4), implies that this is intrinsic to the source rather than the effect of extended emission being resolved out at higher frequencies.

Extrapolating the 1.3 and 2.4 GHz observations gives a flux density of ~3 mJy at 5 GHz. Combining this with the *IRAS* 60 μm flux density of 1.23 Jy (Knapp *et al.* 1989) suggests that NGC 5266 lies close to the FIR-radio relation for spiral galaxies (de Jong *et al.* 1985), and hence that most or all of the radio continuum emission may arise from star-forming regions. It therefore appears that NGC 5266 does not have an active nucleus.

4. RESULTS

4.1 Distribution and Kinematics of the H I in NGC 5266

The neutral hydrogen in NGC 5266 is very extended, as Fig. 3(a) shows. Perhaps the most striking feature is that the H I is elongated along P.A.~135°, i.e., nearly perpendicular to the orientation of the dust lane (P.A.~21°). In most dust-lane and polar-ring galaxies where H I is observed, it lies in the same plane as the dust lane or ring, but NGC 5266 is a rare exception (Morganti *et al.* 1996).

The total extent of the H I in NGC 5266 is ~16′: ~9′ (~160 kpc) on the SE side (corresponding to ~9 times the optical half-light radius R_e) and ~7′ (~120 kpc) on the NW side ($\sim 7R_e$). The large extent of the neutral gas compared to the brightest part of the optical image is evident from Fig. 3(b).

The H I distribution is quite clumpy (clearly seen in Fig. 3(a) and in the channel maps in Fig. 2), but the overall structure has an elliptical shape with a radius of ~4′ in P.A. ~110°. Two thin, arm-like structures extend further out from the main body, the SE arm being somewhat longer than the NW arm. The emission is brighter on the SE side; to the NW the emission is fainter and there is also a hole in the H I distribution.

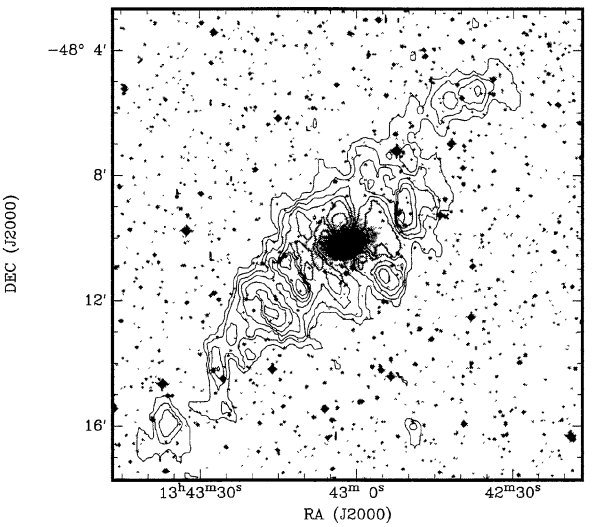

FIG. 3. Map of total H I distribution in NGC 5266 superimposed to the optical image from the Sky Survey. The large extent of the neutral gas compared to the brightest part of the optical image is clear. The contour levels go from 3×10^{19} atoms cm^{-2} to 38×10^{19} atoms cm^{-2} in steps of 5×10^{19} atoms cm^{-2}.

The overall H I velocity field (Fig. 4) is quite regular, and implies that the main H I component of NGC 5266 is a rotating disk roughly perpendicular to the dust lane. The velocity field is not perfectly symmetrical — the kinematical position angle in the western half of the disk is roughly 110°, while in the eastern half of the disk it is closer to 135°. This may mean that the H I in NGC 5266 is not completely settled, though it could also be a result of the clumpy density distribution.

Interestingly, a high-contrast optical image of NGC 5266

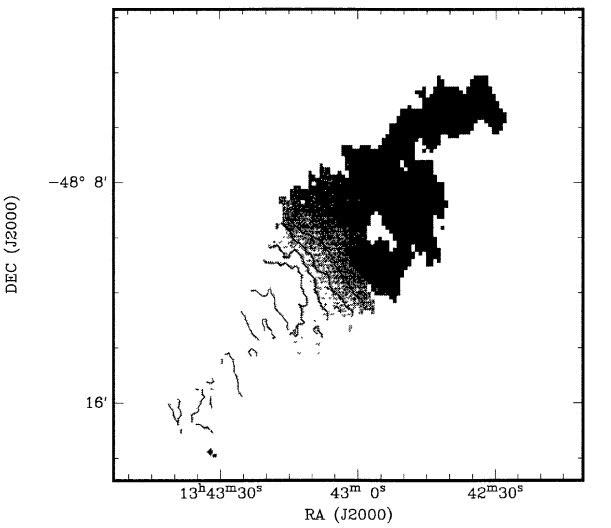

FIG. 4. The intensity-weighted mean H I velocity in NGC 5266. The contours are spaced by 40 km s^{-1} from 2500 to 3400 km s^{-1}. The greyscale also represents the velocity field for the same range of values.

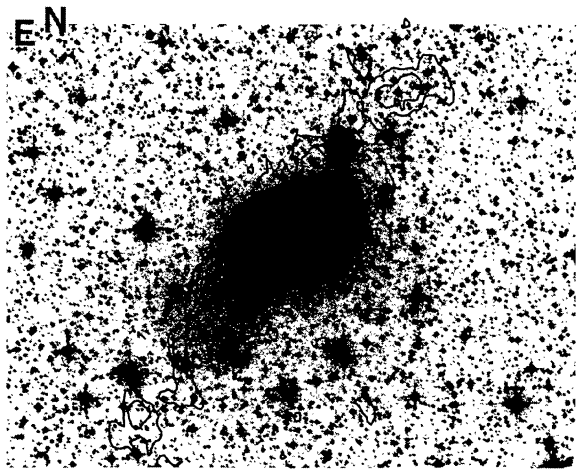

FIG. 5. Total H I (contours) superimposed to a deep optical image (grey).

presented by Caldwell (1984) shows that at very large radii the stellar major axis shifts from P.A. 110° to ~135°, i.e., it shows the same characteristics as the H I. Figure 5 shows our H I total-intensity image superimposed on a high-contrast photograph kindly provided by D. Malin. The faintest optical isophotes correspond well with the main (elliptical-shaped) neutral gas structure, implying that the main H I disk has a faint optical counterpart (see also Sec. 5).

The position-velocity map at P.A. 135° (Fig. 6) shows the signatures of three distinct structures. The first is a central fast-rotating component associated with the dust lane (see below), while the second is the main H I disk which can be traced out to a 4′ radius. The third corresponds to the two outermost arm structures. Here, there is a smooth trend from

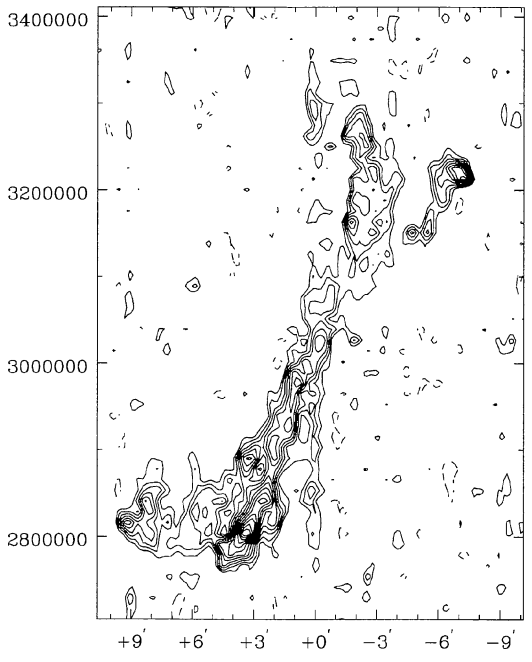

FIG. 6. Position-velocity map obtained from a slice in P.A.=135° and width 90″. The contour levels are −11,11 to 80 mJy beam^{-1} in steps of 6 mJy beam^{-1}.

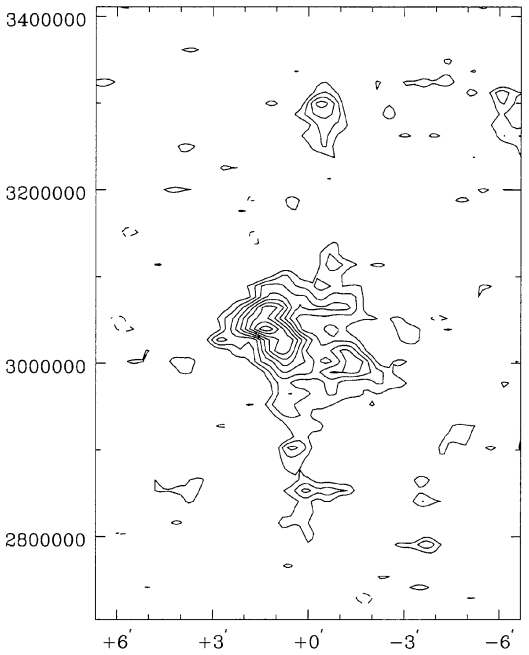

FIG. 7. Position-velocity map obtained from a slice along the minor axis (P.A. 21°) and width 60″. The contour levels are −8, 8 to 40 mJy beam^{-1} in step of 4 mJy beam^{-1}.

one extreme velocity to the other, similar to the behavior expected for an edge-on ring. The large differences in the kinematics of the two sides, however, suggest that this gas may actually be in tidal arms rather than a settled ring.

There are clear hints that some fast-rotating H I is associated with the optical dust lane. High-velocity gas in the central region is clearly visible in the position-velocity plot along the minor axis (P.A.~21°, Fig. 7). Here there is gas at the systemic velocity, plus a fast-rotating component which appears to be spatially resolved along the galaxy's minor axis. The western side of this structure is redshifted compared to the systemic velocity, i.e., it rotates in the same sense as the ionized gas and CO.

The central, fast-rotating H I gas which we identify with the dust lane could, in principle, be gas further out along the major axis which has been smoothed onto the minor axis by the relatively large beam. The position-velocity map along the major axis (Fig. 6) and the channel maps appear to rule this out. The high-velocity gas near the center is a distinct component, and there is no major-axis H I at the required positions and velocities which could have been smeared onto the minor axis by the ATCA beam. Hence we identify the fast-rotating component near the center as H I associated with the dust lane.

We have estimated the mass of the H I associated with the dust lane by masking in position-velocity maps the H I except for the H I associated with the fast-rotating central component. This estimate is compromised by the fact that the H I of the dust lane partially overlaps with the emission of the main H I disk in the data cube. Nevertheless, we estimate the mass to be about 5%–10% of the total H I mass. This would make the ratio of $M_{H_2}/M_{H\,I}$~1–2 for the region of the dust

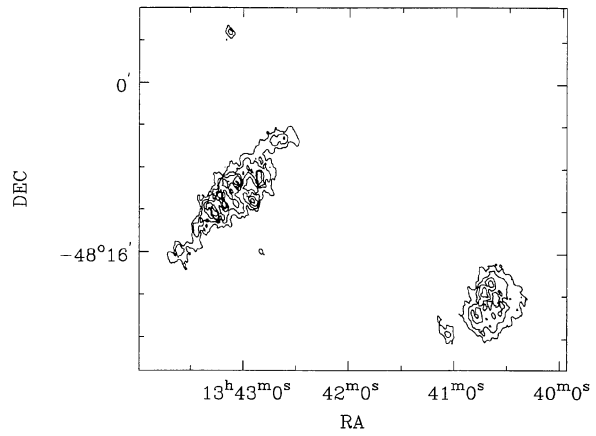

FIG. 8. Total intensity H I emission in the whole field. The contour levels ranges from 3.6×10^{19} atoms cm^{-2} to 36×10^{19} atoms cm^{-2} in step of 7.2×10^{19} atoms cm^{-2}.

lane, very similar to what is observed in some other dust-lane elliptical (Sage & Galletta 1993). The velocity width of the dust-lane H I is also very similar to the width of the CO profile ($\sim$580 km s^{-1}).

4.2 H I Emission from other Galaxies in the Field

NGC 5266 belongs to a small group of galaxies, and we have detected at least three other galaxies within $\sim30'$ of NGC 5266. Figure 8 shows the total H I emission in the whole field, while Table 5 lists the optical positions of NGC 5266 and the detected companion galaxies. There are no obvious signs of interaction between NGC 5266 and any of these galaxies.

The second-brightest galaxy in the field is the large spiral NGC 5266A, which is $\sim27'$ away from NGC 5266, i.e., at a projected distance of $\sim$470 kpc. Although NGC 5266A contains a large amount ($>10^{10}M_\odot$) of H I, we cannot estimate a precise mass because this galaxy lies beyond the half-power point of the ATCA primary beam. Single-dish measurements (Reif *et al.* 1982) suggest an H I mass of $\sim4\times10^{10}M_\odot$.

NGC 5266A has a companion $\sim4'$ to the SE which is visible in Fig. 8. Our observations of the H I emission from this companion were badly affected by the presence of the 1408 MHz interference mentioned above. Only part of the H I profile could be measured since a group of lower-velocity channels had to be flagged because of the interference. Because of this it was not possible to derive an H I mass, and only an indicative number for the systemic velocity is given in Table 5.

We also detected H I emission from the small edge-on spiral ESO 220–G34, which lies $14'$ ($\sim$245 kpc) north of NGC 5266. The 20% width of the H I profile is $\sim$120 km s^{-1}. We derive a total H I mass of $\sim6\times10^8M_\odot$ for this object. For the dynamical mass inside R_{25} we find $\sim5\times10^9M_\odot$, so this appears to be a low-mass spiral companion to NGC 5266.

There is a possible detection of very weak H I emission to the south of NGC 5266, coincident with a small anonymous galaxy. No H I emission was detected from the object noted by Caldwell (1984) in the NW halo of NGC 5266, suggesting that it may be a background object.

4.3 Simple Modeling of the H I Emission

The results described in Sec. *4.1* suggest that the neutral hydrogen inside $4'$ lies in two perpendicular disks. Here we investigate this possibility in somewhat more detail.

We have not attempted any detailed modeling of the H I kinematics (such as a full fit of a tilted-ring model), both because the observed asymmetry of the velocity field suggests that the gas may not be completely settled, and because of the clumpiness of the gas distribution. Instead, we took a simpler and more qualitative approach which minimized the number of free parameters. We argue that the observations are consistent with a model in which NGC 5266 has two orthogonal H I disks, and derive some basic properties.

In modeling the H I kinematics, we assume that the neutral gas in the inner regions is coincident with the dust lane, but that somewhere further out it shifts to a perpendicular plane. The transition from one plane to the other is quite abrupt, though there is evidence in the H I velocity field for a small amount of gas "connecting" the outer region of the optical dust band and the inner part of the main H I disk [see, e.g., the channels at velocities around 2830 and 3280 km s^{-1} and the central part of the total intensity map in Fig. 3(a)]. The transition radius appears to be about $60''$, i.e., the transition lies just beyond the optical dust lane.

Because of the low spatial resolution of our H I observations, we assume that the inner H I disk has the same orientation as the dust lane, i.e., a position angle $i_{\rm inner}=21°$ and an inclination $i_{\rm inner}\sim74°$ (Varnas *et al.* 1987).

For the main disk, we derive an inclination $i_{\rm main}=60-65°$ from the observed axis ratio of the H I contours within a $4'$ radius. The observed position angle at this radius, $\phi_{\rm main}\sim110°$ (Sec. *4.1*) is consistent with the value of 111° expected if the two disks are orthogonal. It is also very close

TABLE 5. Galaxies in the NGC 5266 field.

Object Name	Type	B (mag)	RA (J 2000.0)	Dec (J 2000.0)	$M_{\rm H\,I}$ ($M_\odot$)	$V_{\rm hel}$ (km s^{-1})	W_{20} (km s^{-1})
NGC 5266A	SBcd	12.7	13 40 37.1	−48 20 34	$\sim4\times10^{10}$	2835	220
NGC 5266A comp			13 41 04.0	−48 23 35	*	2650*	
A1342–4816			13 42 49.0	−48 16 3	$\sim2\times10^8$	3245	~70
NGC 5266	E4	12.0	13 43 01.6	−48 10 12	2.4×10^{10}	2990	650
ESO 220–G034	S...	16.6	13 43 06.3	−47 55 24	6×10^8	2960	~120

*Very uncertain due to strong interference, see text.

to the position angle of the stellar major axis (Caldwell 1984; Varnas *et al.* 1987), consistent with the idea that the main H I disk has settled in a symmetry plane of the stellar galaxy. The presence of the inner H I disk means that the main disk must have a central hole of $\sim 2'$ diameter.

To compare this simple model with our data, we used a software package for interactive modeling which is being developed at the ATNF by one of us (TO). This computes a full model cube and allows interactive changes to the model parameters, direct inspection of the resulting cube and a direct comparison with the data cube. Given the nature of our model (i.e., two perpendicular disks) and the clumpiness of the gas distribution, it is important to compare the model cube with the data cube instead of comparing velocity fields. The quality of a model was judged by eye. Although this is subjective, it seems the only sensible way to proceed. The gas was assumed to be moving on circular orbits.

If we assume the rotation velocity to be constant with radius, we find the best fit for $V_{\rm rot}=270$ km s^{-1}, which is close to the values determined optically and from CO observations. For this model, we get a reasonable description of the gas inside $4'$, although the model velocities are slightly higher than those observed on the western edge of the main disk (there is a good fit on the eastern side). The velocities at the eastern edge of the main disk are higher than at the western side and correspond much better to a flat rotation curve.

The fact that a flat rotation curve out to (at least) 4 R_e is reasonably consistent with the data suggests that NGC 5266 may have a dark halo, so it is interesting to see whether models with a declining rotation curve can also fit the data. To do this, we computed models with a larger inclination for the main disk. The maximum inclination of the main disk for which the model remains reasonably consistent with the observations is about 75°, suggesting that the rotation velocity at $4'$ is unlikely to be lower than 250 km s^{-1}. We also investigated models with a slightly falling rotation curve for inclinations around 60°, and again found that the rotation velocity at the edge of the main disk cannot be much smaller than 250 km s^{-1}.

Figure 9 shows some position-velocity plots of slices through the data and model cubes. Figure 9(a) shows a slice at position angle 110° (major axis), Fig. 9(b) shows four slices made at constant RA (i.e., north–south) on both sides of the nucleus and, finally, Fig. 9(c) shows four slices at constant declination (i.e., east–west). These plots confirm that a simple two-disk model fits the observed behavior of the H I. Both the kinematics of the main H I disk and the high-velocity component near the center are described quite well. However, these plots also show that the gas distribution is quite clumpy and asymmetric and that it is impossible to derive a rotation curve accurately. Nevertheless, although we have compared the data with only a relatively simple model, the good agreement between model and data in the inner $4'$ suggests that the H I inside $4'$ is indeed mainly concentrated in two perpendicular planes, and that the rotation velocity does not decrease much from the center to a radius of $4'$.

The H I emission from the outermost regions ($>4'$) cannot be reproduced by our simple model. This is not only because the gas position angle shifts outside $4'$, but because

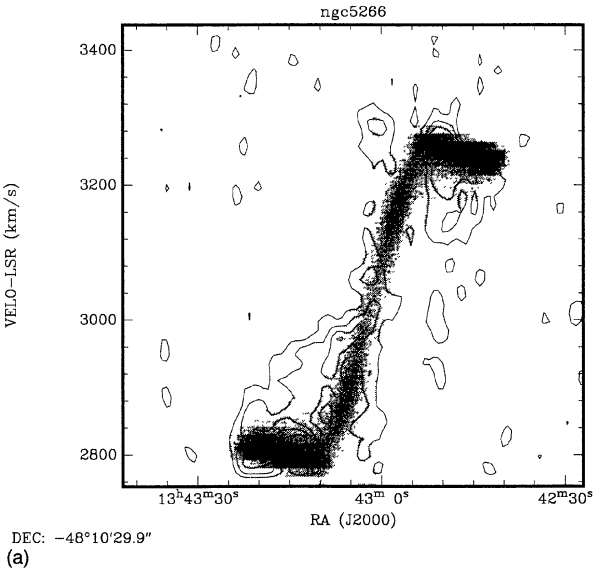

FIG. 9. Comparison of the data (contours) with the simple model (grey) described in Sec. *4.3*: (a) slice in P.A. 110° (major axis), (b) slices made at constant right ascension on both side of the nucleus, and (c) slices made at constant declination.

the overall kinematics suggest a separate structure. We are therefore left with two possibilities, as mentioned earlier.

The outer parts might be tidal tails of neutral gas formed in a merger, and therefore very unrelaxed structures (see also Sec. 5). Alternatively, they could be part of an outer, edge-on disk or ring, as some characteristics of their velocity field seem to suggest (Fig. 6). We note, however, that the velocity amplitude of these outer structures is very similar to the inner H I. More sophisticated modeling (or numerical simulations) will be necessary to investigate the real nature of these structures in more detail.

4.4 Dark Matter in NGC 5266

The flat rotation curves observed for the neutral gas at large radii in spiral galaxies imply that many of these galaxies are surrounded by dark, massive halos. Since very few elliptical galaxies have extended gas disks, the gas disk in NGC 5266 offers a rare opportunity to probe the mass distribution in the outer parts of a large elliptical galaxy by the same techniques used for spirals.

Using the model described above, we can estimate the mass-to-light ratio within about $4'$ from the center of NGC 5266, i.e., the region within which we feel confident that the gas lies in a settled disk. Assuming a constant rotation velocity of 270 km s^{-1} and a spheroidal mass distribution with an intrinsic flattening of $q=0.6$ as indicated by the optical image of the galaxy, we can derive the mass of the galaxy within this radius. Adopting an $r^{1/4}$ law light profile with $R_e=65''$ (Varnas *et al.* 1987), we find that the derived mass-to-light ratio ranges from $M/L_B \sim 4$ at $1'$ radius to $M/L_B=8$ at $4'$. Adopting a spherical rather than a flattened mass distribution would increase these values by $\sim 20\%$.

Comparing our derived values with that measured for the central M/L_B from optical observations ($M/L_B=3.0$ at 0.3

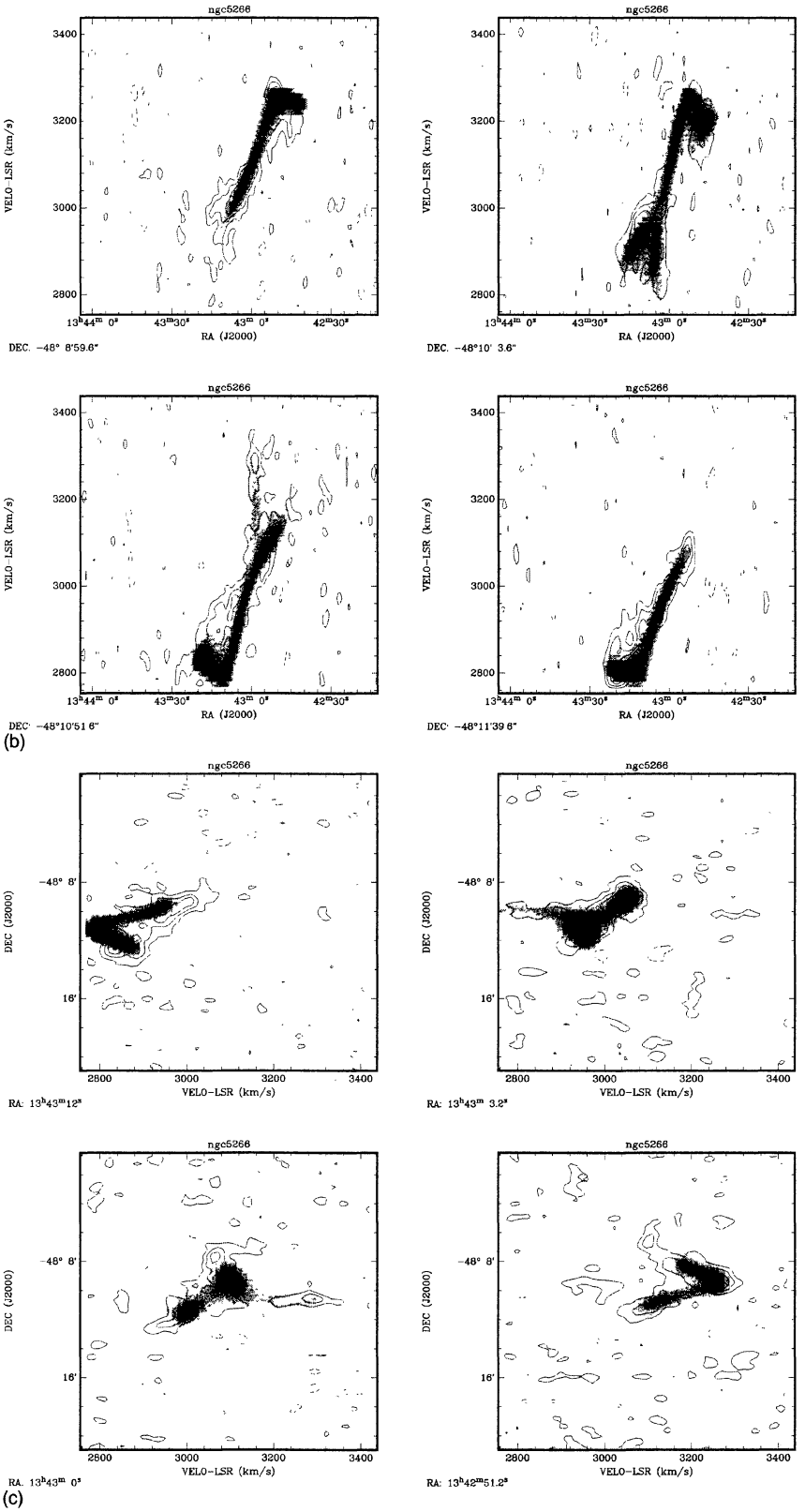

FIG. 9. (continued)

R_e, Bertola *et al.* 1993), we find that M/L_B increases by a factor ~ 2.7 between the center and $r = 4\,R_e$.

If we use the outermost H I to estimate the mass-to-light ratio beyond a 4′ radius, we derive $M/L_B \sim 16$ within an 8′ radius. However, as discussed earlier, it is likely that the two outer H I structures are not in equilibrium. If so, this value should be disregarded.

In summary, we find reasonable evidence for dark matter in NGC 5266 at a radius of $4\,R_e$. The values of M/L_B found in NGC 5266 are close to those measured in the few other elliptical galaxies which have reliable M/L_B estimates in their outer regions. One of the best cases for a radial increase of M/L is in IC 2006. Schweizer *et al.* (1989) and Franx *et al.* (1994) have used the H I ring around this object to derive an integrated M/L_B of 16 out to $6.5\,R_e$, compared to $M/L_B = 5$ for the inner regions. A similar increase of M/L_B with radius has been also recently shown by a study of the mass distribution in the elliptical galaxy NGC 5128 by using planetary nebulae (Hui *et al.* 1995). In the case of NGC 5128, M/L_B increases from 3.9 in the inner part to 10 in the outer regions ($\sim 5\,R_e$), consistent with what is found from the neutral hydrogen data (Schiminovich *et al.* 1994).

Figure 10 (modified from Bertola *et al.* 1993) summarizes these numbers and includes the new results for NGC 5266. The solid line represents the cumulative M/L_B as a function of radius for spiral galaxies as discussed by Bertola *et al.* (1993). The superimposed points represent ellipticals. NGC 5266 falls well within the region characteristic of spiral galaxies (as do the other ellipticals), in agreement with the suggestion of Bertola *et al.* (1993) of a parallel behavior of dark matter in ellipticals and spiral galaxies.

It is interesting that, at very large radii, the relation for spiral galaxies in Fig. 10 approaches values consistent with $0.2 \leqslant \Omega \leqslant 0.3$, which is now considered typical for groups and clusters (David *et al.* 1995). If elliptical galaxies have similarly large M/L at radii beyond so far measured, it would suggest the remarkable result that most of the dark matter observed in the universe may lie in the massive halos of spiral and elliptical galaxies. A similar suggestion (based on X-ray observations) has also been made by Bahcall *et al.* (1995).

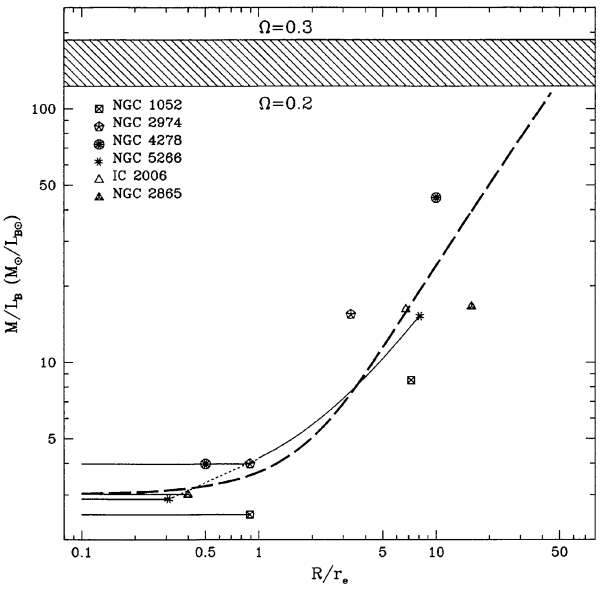

FIG. 10. The $\log(M/L_B)$–$\log(R/R_e)$ diagram. The dashed thick line represents the cumulative M/L_B as a function of radius for spiral galaxies shifted in the central part for a factor to match the M/L of ellipticals (from Bertola *et al.* 1993). The symbols represent the data for the ellipticals obtained from optical and H I data and the full line represents the M/L radial profile of NGC 5266 derived in the present paper. The shaded region represents the typical M/L of groups and clusters.

5. THE ORIGIN OF THE GAS DISK IN NGC 5266

The two orthogonal gas disks in NGC 5266 probably represent the two stable planes for gas (one perpendicular to the longest axis and one perpendicular to the shortest axis, (Steiman-Cameron 1984; Heiligman & Schwarzschild, 1979) characteristic of a triaxial galaxy with a stationary potential.

Although most of the H I lies in these two planes, there are some hints in the data that the two disks might be part of a single warped structure. If so, NGC 5266 would resemble some of the classical warps such as NGC 3718 (Schwarz, 1985) or NGC 660 (Gottesman & Mahon 1990; Arnaboldi & Galletta 1993), though with the important difference that relatively little gas is found at intermediate radii. Possibly this means that the warp is "breaking up" into two disks.

Further support for the presence of a warp comes from the warped shape of the optical dust lane. As mentioned in Sec. 2, the origin of this warp has been discussed by Caldwell (1984) and Varnas *et al.* (1987). Moreover, most of the gas appears to be settled and this could argue in favor of the hypothesis of a warp formed by the figure slowly tumbling, as suggested by Varnas *et al.* 1987. Since the gas motion in the main disk is prograde with respect to the stellar streaming, this implies that the figure rotation must be retrograde (Van Albada *et al.* 1982; Bertola *et al.* 1985). However, the initial conditions used by Varnas *et al.* in their simulations are probably not representative of the whole H I disk in NGC 5266: it is unlikely that the gas was initially in one coplanar disk (see below), and the true initial size of the neutral gas distribution must have been much larger than assumed by Varnas *et al.*

There are some similarities between the H I distribution in NGC 5266 and NGC 5128 (Centaurus A). In the latter, most of the H I is associated with the dust lane, but at large radii the H I has a different kinematical behavior and forms a partial ring, highly inclined to the dust lane (Schiminovich *et al.* 1994).

A puzzling feature of NGC 5266 is the origin of the huge amount of H I. It is generally believed that the H I in elliptical galaxies has an external origin (e.g., Knapp *et al.* 1985), particularly since the kinematics of the gas and the stars are often very different. However, the amount of neutral gas in NGC 5266 is unusually large for an early-type galaxy (Knapp *et al.* 1985), and almost certainly larger than could have been provided by an infalling small companion galaxy. A similar amount of H I has recently been detected in the radio galaxy PKS B1718-649 (Véron-Cetty *et al.* 1995). In this object, faint spiral structure has been detected and a

likely interpretation is that the gas comes from a merger involving one or two luminous spirals.

It is interesting to compare the optical and H I properties of NGC 5266 with the typical values for 'normal' elliptical and spiral galaxies compiled by Roberts & Haynes (1994). The optical luminosity ($L_B = 10^{11} L_\odot$) and color ($B-V = 0.97$; Sadler 1984b) of NGC 5266 are typical of elliptical galaxies; but the total H I mass ($2.4\times10^{10} M_\odot$) is not only high for an early-type galaxy, but exceeds that in most bright spirals (the median H I mass in the Roberts & Haynes RC3–UGC sample is around $1.5\times10^{10} M_\odot$ for Sb and Sc spirals, and $1.2\times10^{9} M_\odot$ for E/S0 galaxies with detected H I). The ratio of the total hydrogen mass to the total (blue) luminosity in NGC 5266 is $M_{\rm H\,I}/L_B \sim 0.2$, which again is a typical value for spiral galaxies but much higher than seen in most ellipticals.

If NGC 5266 is indeed the result of a merger, it seems likely that two gas-rich spiral galaxies must have been involved in order to provide the large H I mass which remains. Furthermore, a large amount of neutral gas must have survived the collision without forming stars.

Toomre & Toomre (1972) originally suggested that elliptical galaxies could form through the merger of two spirals. Many follow-up studies, both theoretical and observational, have shown that such a merger can lead to an $r^{1/4}$ law for the final stellar remnant (see Barnes & Hernquist 1992). The morphology and the kinematics of the H I in NGC 5266 also support a picture in which the galaxy formed by a merger of two gas-rich spirals.

Numerical simulations of the merging of two spirals (Hibbard & Mihos 1995) show that there are two phases in the evolution of the gas in such mergers. Initially, a significant fraction of the gas piles up in the center and fuels a burst of star formation. The remaining gas is in tidal arm-like structures at larger radii. Later, there is slow infall of "returning" gas from these tidal features and this gas can settle, depending on the starting conditions, in a disk or a ring. Hibbard & Mihos have shown that this second phase is important, e.g., in the merger remnant NGC 7252. Their model for the future evolution (> 1.2 Gyr) of this galaxy has a similar gas morphology to that observed in NGC 5266, i.e., part of the H I is settling in the galaxy while the tidal arms are also still present. It seems likely that NGC 5266 is a similar system to NGC 7252, but at a later stage in its evolution.

The correspondence between the faint optical outer isophotes and the H I gas is also interesting in this respect. As already mentioned in Sec. *4.1* and shown in Fig. 5 a faint stellar extension some 3′–4′ can be seen on either side of the nucleus, which Caldwell (1984) already interpreted as possible shells like those seen in many early-type galaxies. Schiminovich *et al.* (1994, 1995) have drawn attention to a possible association between the optical shells and features in the H I distribution in some shell galaxies. Such an association is not expected in the standard accretion model for the formation of the optical shells, since the gas and the stars would separate at an early stage in the accretion event, caused by the effects of dissipation on the gas. However, if secondary infall is important, as is possibly the case in NGC 5266, association between faint optical features and H I may occur. Since the gas in the tidal arms has mainly been orbiting around the galaxy, dissipational effects are not too important and the gas should still be reasonably coincident with the stars from the tidal arms.

TABLE 6. Comparison of NGC 5266 with "starburst" mergers.

	Peak starburst	NGC 7252	NGC 5266
$L_{\rm FIR}/M_{\rm H_2}$	~80	11.4	6.3
$L_{\rm FIR}/L_B$	~60	0.9	0.2
$T_{60/100\ \mu\rm m}$	~50 K	37 K	30 K
Reference	a	b	c

References: (a) Casoli *et al.* 1991, (b) Dupraz *et al.* 1990, (c) This paper.

How reliably can we date the merger event which gave rise to NGC 5266? Hibbard & Mihos (1995) find the best match between their model and the data at $t \sim 1.2$ Gyr, so this is a lower limit if we believe that NGC 5266 is more evolved than NGC 7252. Two further pieces of evidence may be helpful: the current rate of star formation is low, and the galaxy does not appear to host an active nucleus.

Mergers between two gas-rich spirals are believed to give rise to ultraluminous *IRAS* galaxies, though the ultraluminous starburst phase is a relatively short-lived one (of duration $\sim 10^8$ yr, whereas the tidal tails can persist for a few times 10^9 yr). An evolutionary sequence has been proposed (Joseph & Wright 1985; Casoli *et al.* 1991) for the merger of gas-rich systems in which (after a period of high activity with rapid star formation) the system returns to a "normal" level and the IR luminosity also returns to normal. The IR characteristics of NGC 5266 fit such a theory. Table 6 compares several of the indicators used by Casoli *et al.* [$L_{\rm FIR}/M_{\rm H_2}$, which is a measure of star-forming efficiency; $L_{\rm FIR}/L_B$; and the temperature derived from the 60/100 μm flux ratio $T_{60/100\ \mu\rm m}$, which indicates how much the dust is heated by a starburst (see Solomon & Sage 1988)] for the most active starburst galaxies, and for NGC 7252 and NGC 5266. This again suggests that NGC 5266 lies beyond NGC 7252 right at the end of the evolutionary sequence, identifying it as an old merger. In summary, the properties of NGC 5266 listed in Table 6 are consistent with a scenario in which the galaxy formed by the merger of two gas-rich spirals

Since NGC 5266 contains such a large amount of neutral gas, it is natural to ask why this gas is not currently forming stars. In other words, why does the optical body of NGC 5266 resemble an elliptical galaxy rather than a spiral? The answer is probably that the surface density of H I gas is currently too low to support star formation.

Kennicutt (1989) has shown that there is a threshold gas density above which star formation occurs, and points out that the H I disks seen in S0 galaxies generally fall below this threshold. Figure 11 plots the radially averaged HI surface density in NGC 5266. The peak value is $\sim 1.3\ M_\odot/{\rm pc}^2$, which is well below that for most spiral disks ($4-8\ M_\odot/{\rm pc}^2$; e.g., Cayatte *et al.* 1994). The H I surface density is well below Kennicutt's star-formation threshold throughout NGC 5266. Our H I data are therefore consistent with other evidence that there has been little or no recent star-formation outside the nucleus of NGC 5266.

There is, however, at least circumstantial evidence that

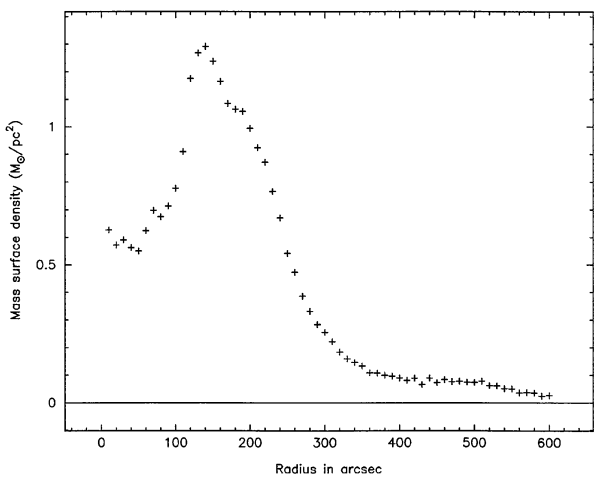

FIG. 11. Plot of the azimuthally averaged H I surface density in NGC 5266.

some star formation is taking place in the innermost regions. The evidence includes the observations that: (i) NGC 5266 obeys the FIR-radio relation for spirals, which is believed to be driven by star formation, (ii) the radio continuum emission comes from within the central 3–5 kpc, (higher-resolution continuum observations could provide more stringent limits), and (iii) the observed radio spectral index of -1.0 is consistent with emission from star-forming regions. Optical/IR spectroscopy with good spatial resolution would be the best way to determine the central star-formation rate directly. In most spiral galaxies, the *IRAS* 60 μm flux arises from a region no larger than the associated radio continuum emission (e.g., Bicay & Helou 1990). If this is also the case in NGC 5266, then the *IRAS* emission arises from the inner 15 arcsec, which is less than the diameter of the dust-lane. Star formation may therefore be very localized.

As in most cases where a dust-lane elliptical is studied, the obvious parallel that is drawn is with Centaurus A. There are many geometrical similarities in the optical and neutral gas between the two objects, so why is NGC 5128 a radio galaxy when NGC 5266 not?

The infall model in which clouds of cold gas from a disk are accreted to the center and fuel the nuclear engine was first proposed by Gunn (1979). This idea is supported by the results of van Gorkom *et al.* (1989), who found redshifted H I absorption (i.e., indicating infall) against the nucleus of several radio galaxies. The modest infall rate required can be easily provided by the small amount of gas present in the inner regions of "normal" ellipticals, and Jaffe *et al.* (1993) point out that although large-scale dust, disks and filamentary structures can be statistically correlated with the nuclear activity, gas on much smaller scales (a few parsecs) is responsible for the actual fueling of the "monster."

In this picture, the huge amount of neutral gas observed in NGC 5266 may be irrelevant to the fueling of an active nucleus, simply because it is too far away. There are a number of possible theories. The first is that NGC 5266 is not active because very little gas has reached the central regions. If so, the initial parameters of the merger may be critical in determining whether or not the gas is driven into the center. NGC 5266 might still host an AGN in the future if gas from the second, slow infall phase falls into the nucleus. A second, and perhaps more likely, theory, is that NGC 5266 has had an AGN in the past, but that activity has now stopped because the central gas supply has been exhausted and no more gas has moved into the center to take its place.

On the other hand, the radio power of NGC 5266 is quite typical for elliptical galaxies of similar optical luminosity, while stronger radio sources (like NGC 5128) are usually found in galaxies of larger optical luminosity (Sadler *et al.* 1989). If the properties or presence of the compact nucleus (or black hole) correlate with galaxy mass, the absence of an active nucleus in NGC 5266 is perhaps not surprising.

6. CONCLUSIONS

We have presented the first H I images of the gas-rich elliptical galaxy NGC 5266. We find that the gas in this galaxy lies in two orthogonal disks; some H I is associated with an inner, minor-axis dust lane but most lies in an extended, outer disk aligned with the stellar major axis. Using the main disk as a mass tracer, we find a mass-to-light ratio $M/L_B \sim 8$ within $4R_e$ and possibly increasing to a value of 16 at a radius of $8R_e$. This increase of M/L state with radius is similar to that derived for other ellipticals and suggests the presence of dark matter.

The most likely origin for NGC 5266 appears to be the merger of two gas-rich spirals, and the settled nature of the gas suggests that this probably occurred at least 1.2 Gyr ago. Unlike some other gas-rich ellipticals, NGC 5266 does not have an active nucleus.

We thank Renzo Sancisi for his useful comments and David Malin for kindly providing the deep optical image. AP acknowledges support from a *Acciaierie Beltrame* grant. This research has made use of the NASA/IPAC Extragalactic Database (NED) which is operated by the Jet Propulsion Laboratory, Caltech, under contract with the NASA.

REFERENCES

Allen, R. J., Ekers, R. D., & Terlouw, J. P. 1985, in Proceedings of the International Workshop on Data Analysis in Astronomy, edited by L. Scarsi and V. di Gesù (Plenum, London), p. 271
Arnaboldi, M., & Galletta, G. 1993, A&A, 268, 411
Bicay, M. D., & Helou, G. 1990, ApJ, 362, 59
Bahcall, N. A., Lubin, L. M., & Dorman, V. 1995, ApJ, 447, 81
Barnes, J. E., & Hernquist, L. E. 1992, ARA&A, 30, 705
Bertola, F., Pizzella, A., Persic, M., & Salucci, P. 1993, ApJ, 416, L45
Bertola, F., Galletta, G., & Zeilinger, W. W. 1985, ApJ, 292, L51
Caldwell, N. 1984, ApJ, 278, 96
Casoli, F., Dupraz, C., Combes, F., & Kazès, I. 1991, A&A, 251, 1
Cayatte, V., Kotanyi, C., Balkowski, C., & van Gorkom, J. H. 1994, AJ, 107, 1003
David, L. P., Jones, C., & Forman, W. 1995, ApJ, 445, 578
de Jong, T., Klein, U., Wielebinski, R., & Wunderlich, E. 1985, A&A, 147, L6

de Vaucouleurs, G., *et al.* 1991, Third Reference Catalogue of Bright Galaxies (Springer, Berlin)
de Zeeuw, T., & Franx, M. 1991, ARA&A, 29, 239
de Zeeuw, P. T. 1992, in Morphological and Physical Classification of Galaxies, edited by G. Longo, M. Capaccioli, and G. Busarello (Kluwer Academic Publisher, Dordrecht), p. 139
Dupraz, C., Casoli, F., Combes, F., & Kazès, I. 1990, A&A, 228, L5
Franx, M., van Gorkom, J. H., & de Zeeuw, T. 1994, ApJ, 436, 642
Goudfrooij, P., de Jong, T., Hansen, L., & Norgaard-Nielsen, H. U. 1994, MNRAS, 271, 833
Gottesman, S. T., & Mahon, M. E. 1990, in Paired and Interacting Galaxies, edited by J. W. Sulentic, W. C. Keel, and C. M. Telesco (NASA, Washington D.C.), p. 209
Gunn, J. E. 1979, in Active Galactic Nuclei, edited by C. Hazard and S. Mitton (Cambridge University, Cambridge), p. 213
Harnett, J. I. 1987, MNRAS, 227, 887
Heiligman, G., & Schwarzschild, M. 1979, ApJ, 233, 872
Hibbard, J. E., & Mihos, J. C. 1995, AJ, 110, 140
Hui, X., Ford, H. C., Freeman, K., & Dopita, M. 1995, ApJ, 449, 592
Jaffe, W., Ford, H. C., Ferrarese, L., van den Bosch, F., & O'Connell, R. W. 1993, Nature, 364, 213
Joseph, R. D., & Wright, G. S. 1985, MNRAS, 214, 87
Kennicutt, R. C. 1989, ApJ, 344, 685
Kotanyi, C., & Ekers, R. D. 1979, A&A, 73, L1
Knapp, G. R., Turner, E. L., & Cunniffe, P. E. 1985, AJ, 90, 454
Knapp, G. R. 1986, in Structure and Dynamics of Elliptical Galaxies, IAU 127, edited by T. de Zeeuw (Kluwer, Dordrecht), p. 145
Knapp, G. R., Guhathakurta, P., Kim, D.-W., & Jura, M. 1989, ApJS, 70, 329
Morganti, R., Sadler, E. M., & Oosterloo, T. 1996, in Second Stromlo Symposium: The Nature of Elliptical Galaxies, edited by M. Arnaboldi, G. S. Da Costa, and P. Saha, ASP Conf. Ser. (in press)
Möllenhoff, C., Hummel, E., & Bender, R. 1992, A&A, 255, 35
Reif, K., Mebold, U., Goss, W. M., Van Woerden, H., & Siegman, B. 1982, A&AS, 50, 451
Roberts, M. S., Hogg, D. E., Bregman, J. N., Forman, W. R., & Jones, C. 1991, ApJS, 75, 751
Roberts, M. S., & Haynes, M. P. 1994, ARA&A, 32, 115
Sadler, E. M. 1984a, AJ, 89, 53
Sadler, E. M. 1984b, AJ, 89, 34
Sadler, E. M., & Gerhard, O. E. 1985, MNRAS, 214, 177
Sadler, E. M., Jenkins, C. R., & Kotanyi, C. 1989, MNRAS, 250, 591
Sage, L., & Galletta, G. 1993, ApJ, 419, 544
Sault, R. J., Teuben, P. J., & Wright, M. C. H. 1995, in Astronomical Data Analysis Software and Systems IV, edited by R. Shaw, H. E. Payne, and J. J. E. Hayes (ASP Conf. Ser. 77 (ASP, San Francisco), p. 433
Schiminovich, D., van Gorkom, J. H., van der Hults, J. M., & Kasow, S. 1994, ApJ, 423, L101
Schiminovich, D., van Gorkom, J. H., van der Hults, J. M., & Malin, D. F. 1995, ApJ, 444, L77
Schwarz, U. J. 1985, A&A, 142, 273
Schweizer, F., van Gorkom, J. H., & Seitzer, P. 1989, ApJ, 338, 770
Solomon, P. M., & Sage, L. J. 1988, ApJ, 334, 613
Solomon, P. M., Rivolo, A. R., Barrett, J. W., & Yahil, A. 1987, ApJ, 319, 730
Steiman-Cameron, T. Y. 1984, Ph.D. dissertation, Indiana University
Toomre, A., & Toomre, J. 1972, ApJ, 178, 623
van Albada, T. S., Kotanyi, C. G., & Schwarzschild, M. 1982, MNRAS, 198, 303
van Dokkum, P. G., & Franx, M. 1995, AJ, 110, 2027
van Gorkom, J. H., Knapp, G. R., Ekers, R. D., Ekers, D. D., Laing, R. A., & Polk, K. S. 1989, AJ, 97, 708
van Gorkom, J. H., & Ekers, R. D. 1989, in Synthesis Imaging in Radio Astronomy, edited by R. A. Perley, F. R. Schwab, and A. H. Bridle, ASP Conf. Ser. 6, (ASP, San Francisco), p. 341
van Gorkom, J. H. 1992, in Morphological and Physical Classification of Galaxies, edited by G. Longo, M. Capaccioli, and G. Busarello (Kluwer Academic Publisher, Dordrecht), p. 233
Varnas, S. R., Bertola, F., Galletta, G., Freeman, K. C., & Carter, D. 1987, ApJ, 313, 69
Véron-Cetty, M.-P., Woltjer, L., Ekers, R. D., & Staveley-Smith, L. 1995, A&A, 297, L79